43rd AIAA Aerospace Sciences Meeting and Exhibit, January 10–13, 2005 Reno, Nevada

Time Spectral Method for Periodic Unsteady Computations over Two- and Three- Dimensional Bodies

Arathi K. Gopinath*, and Antony Jameson†
Stanford University, Stanford, CA 94305-4035

The Time Spectral Algorithm is proposed for the fast and efficient computation of time-periodic turbulent Navier-Stokes calculations past two- and three-dimensional bodies. The efficiency of the approach derives from these attributes: 1)time discretization based on a Fourier representation in time to take advantage of its periodic nature, 2)multigrid to drive a fully implicit time stepping scheme. The accuracy and efficiency of this technique is verified by Euler and Navier-Stokes calculations for a pitching airfoil and a pitching wing. Results verify the small number of time intervals per pitching cycle required to capture the flow physics. Spectral convergence is demonstrated for pitching motion characterised by many frequencies.

I. INTRODUCTION

Computational Fluid Dynamics has been gaining widespread acceptance across disciplines due to continuous reduction in computational costs which stem from both improvements in computer hardware and faster algorithms.

Time dependent calculations find a wide variety of applications including flutter analysis, analysis of flow around helicopter blades in forward flight and rotor-stator combinations in turbomachinery. Typically, explicit time-stepping schemes require the use of very small time steps to obtain reasonable accuracy, whereas implicit schemes allow much larger time steps but are prohibitively expensive for three-dimensional calculations. Unsteady flow calculations of realistic industrial applications continue to be very expensive. On the other hand a state-of-the-art two-dimensional steady inviscid calculation[1] of flow past an airfoil takes very small number of multigrid cycles to converge to reasonable accuracy. Modifying and incorporating such efficient algorithms to suite unsteady computations may be rewarding. Time dependent calculations call for such break-throughs.

When time accurate solvers like the implicit second-order Backward Difference Formula(BDF) are used to treat periodic flows, the governing equations are integrated in time until the periodic steady state is reached. This may require integrations over 5 or more cycles for a typical pitching motion.

This paper proposes the Time Spectral Method to solve time-periodic unsteady problems, following the direction suggested by Hall et.al.[2] Compared to the dual time stepping BDF, applicable for arbitrary time histories, this algorithm promises significant reduction in CPU requirements for time periodic flows. A Fourier representation is used for time discretization, leading to spectral accuracy. Moreover periodicity

*Doctoral Candidate, AIAA Student Member.
†Thomas V. Jones Professor of Engineering, Department of Aeronautics and Astronautics, AIAA Member

is directly enforced and hence the solution does not have to evolve through transients to reach a periodic steady-state. When the equations are transformed back to the physical domain, the time derivative appears as a high-order central difference formula coupling all the time levels in the period. The solution is obtained by marching towards a steady-state in an auxiliary pseudo-time variable, while a multigrid procedure is used to accelerate the convergence of the whole process. The method has been applied to both two- and three-dimensional unsteady flows past moving bodies. Preliminary applications are to pitching airfoils and wings where there is ample ground for validating the algorithm with experimental and other established numerical results.

II. MATHEMATICAL FORMULATION

This section describes the mathematical formulation of the governing equations and the proposed Time Spectral method for time-periodic unsteady calculations.

A. Governing Equations

The Navier-Stokes equations in integral form are given by

$$\int_{\Omega} \frac{\partial w}{\partial t}\, dV + \oint_{\partial\Omega} \vec{F} \cdot \vec{N}\, ds = 0.$$

In semi-discrete form, the unsteady equations in Cartesian coordinates can be written as

$$V\frac{\partial w}{\partial t} + R(w) = 0, \qquad R(w) = \frac{\partial}{\partial x_i} f_i(w), \tag{1}$$

where w is the vector of conserved variables,

$$w = \begin{bmatrix} \rho \\ \rho u_1 \\ \rho u_2 \\ \rho u_3 \\ \rho E \end{bmatrix}$$

and $R(w)$ is the residual vector of spatial discretization representing contributions from both the physical inviscid and viscous fluxes and numerical dissipation fluxes. If the mesh is moving with velocity components u_{1m}, u_{2m} and u_{3m} at each mesh point, the fluxes f_i are given by

$$f_i = f_{ci} - f_{vi},$$

where the convective fluxes f_{ci} and viscous fluxes f_{vi} are defined as

$$f_{ci} = \begin{bmatrix} \rho u_{ir} \\ \rho u_{ir} u_1 + p\delta_{i1} \\ \rho u_{ir} u_2 + p\delta_{i2} \\ \rho u_{ir} u_3 + p\delta_{i3} \\ \rho u_{ir} E + p u_i \end{bmatrix}, \quad f_{vi} = \begin{bmatrix} 0 \\ \tau_{i1} \\ \tau_{i2} \\ \tau_{i3} \\ \vec{u} \cdot \vec{\tau_i} - q_i \end{bmatrix}. \tag{2}$$

Here $u_{ir} = u_i - u_{im}$ and δ is the Kronecker delta.

Turbulent flow is modeled by the Reynolds-Averaged Navier-Stokes(RANS) equations with a turbulence model. $\bar{\bar{\tau}}$ is the stress tensor and its components are given by,

$$\tau_{ii} = 2\mu u_i + \lambda(u_{1,x_1} + u_{2,x_2} + u_{3,x_3}),$$

$$\tau_{ij} = \tau_{ji} = \mu(u_{i,x_j} + u_{j,x_i}).$$

Here $\lambda = \frac{-2}{3}\mu$(by assumption) and the heat flux vector q's components are given by

$$q_i = -\kappa T_i.$$

T_i are temperature gradients and

$$\kappa = \gamma(\frac{\mu_{lam}}{Pr_{lam}} + \frac{\mu_{turb}}{Pr_{turb}}), \mu = \mu_{lam} + \mu_{turb}.$$

μ_{lam} and μ_{turb} are the laminar and turbulent kinematic viscosities, Pr_{lam} and Pr_{turb} are the laminar and turbulent Prandtl numbers.
The equation of state provides the closure. For an ideal gas,

$$p = (\gamma - 1)\rho(E - \tfrac{u_i u_i}{2}), \quad H = E + \tfrac{p}{\rho}. \tag{3}$$

B. Implicit Schemes based on the Backward Difference Formula(BDF)

In order to time accurately solve the unsteady governing equations, the Backward Difference Formula discretizes Eq.1 implicitly as

$$D_t(V^{n+1}w^{n+1}) + R(w^{n+1}) = 0.$$

The operator D_t of k^{th} order accuracy is of the form

$$D_t = \frac{1}{\Delta t}\sum_{q=1}^{k}\frac{1}{q}(\Delta^-)^q,$$

where

$$\Delta^- w^{n+1} = w^{n+1} - w^n.$$

For example, the second-order A-stable BDF scheme is

$$\frac{3w^{n+1}V^{n+1} - 4w^nV^n + w^{n-1}V^{n-1}}{2\Delta t} + R(w^{n+1}) = 0,$$

where Δt is the physical time step. Since we have a rigidly-moving body-fitted mesh, $V^{n+1} = V^n = V^{n-1} = V$. Then,

$$V\frac{3w^{n+1} - 4w^n + w^{n-1}}{2\Delta t} + R(w^{n+1}) = 0.$$

1. *Dual Time Stepping BDF scheme*

Jameson[3] proposed the multigrid dual time stepping BDF that consists of the coupled non-linear equations, and solved them by inner iterations which advance in pseudo-time t^* to steady-state. Hence the scheme solves

$$\frac{\partial w}{\partial t^*} + R^*(w) = 0,$$

where

$$R^*(w) = V\frac{3w^{n+1} - 4w^n + w^{n-1}}{2\Delta t} + R(w^{n+1}).$$

An explicit multistage Runge-Kutta time-marching scheme with variable local Δt^* along with multigrid and residual averaging is implemented. If a large number of inner iterations is required at each physical time step, then the method becomes very expensive and calls for a better algorithm for the inner iterations.

Second order accuracy is guaranteed with the BDF scheme if the inner iterations converge fully. Hsu et. al.[4] have suggested a hybrid scheme that can yield sufficient accuracy without having to converge fully.

C. Time-Spectral Methods

Time periodic unsteady flows are typical in turbomachinery applications. Taking advantage of the periodic nature of the problem, a Fourier representation in time can make it possible to achieve spectral accuracy. Also, if engineering accuracy can be obtained with small number of time intervals, then dramatic reductions in computational time can be achieved.

Recall the semi-discrete form of the governing equations (1),

$$V\frac{\partial w}{\partial t} + R(w) = 0.$$

The discrete fourier transform of w, for a time period T, is given by

$$\hat{w}_k = \frac{1}{N}\sum_{n=0}^{N-1} w^n e^{-ik\frac{2\pi}{T}n\Delta t}$$

and its inverse transform,

$$w^n = \sum_{k=-\frac{N}{2}}^{\frac{N}{2}-1} \hat{w}_k e^{ikn\frac{2\pi}{T}\Delta t}, \tag{4}$$

where the time period T is divided into N time intervals, $\Delta t = T/N$.

Discretize the governing equations as a pseudo-spectral scheme,

$$V D_t w^n + R(w^n) = 0. \tag{5}$$

McMullen et.al.[5,6]solved the time accurate equations in Eq.(5) by transforming them into frequency domain and introducing a pseudo-time t^*, like in the case of the dual time stepping scheme,

$$V\frac{\partial \hat{w}_k}{\partial t^*} + V\frac{2\pi}{T}ik\hat{w}_k + \hat{R}_k = 0.$$

Alternatively, the Time Spectral Algorithm proposes to solve the governing equations in the time-domain, considerably gaining on the computational cost required to transform back and forth to the frequency domain. The method is also easy to implement in an existing steady-state solver without having to deal with complex arithmetic. From Eq.(4), the time discretization operator D_t can be written as

$$D_t w^n = \frac{2\pi}{T}\sum_{k=-\frac{N}{2}}^{\frac{N}{2}-1} ik\hat{w}_k e^{ik\frac{2\pi}{T}n\Delta t}.$$

This summation involving the fourier modes $\hat{w}_k$, can be rewritten in terms of the conservative variables w in the time domain as,[7]

$$D_t w^n = \sum_{j=0}^{N-1} d_n^j w^j$$

where

$$d_n^j = \begin{cases} \frac{2\pi}{T}\frac{1}{2}(-1)^{n-j}cot(\frac{\pi(n-j)}{N}) & : \quad n \neq j \\ 0 & : \quad n = j \end{cases}$$

This representation of the time derivative expresses the multiplication of a matrix with elements d_n^j and the vector w^j. With a change of variables, let $(n-j) = -m$, the time derivative is further rewritten as

$$D_t w^n = \sum_{m=-\frac{N}{2}+1}^{\frac{N}{2}-1} d_m w^{n+m},$$

where

$$d_m = \begin{cases} \frac{2\pi}{T}\frac{1}{2}(-1)^{m+1}cot(\frac{\pi m}{N}) & : \quad m \neq 0 \\ 0 & : \quad m = 0 \end{cases}$$

Note that $d_{-m} = -d_m$. Hence D_t takes the form of a central difference operator connecting all the time levels, yielding an integrated space-time formulation which requires the simultaneous solution of the equations for all time levels. A pseudo-time t^* is introduced as in the dual-time stepping case, and the equations are time marched to a periodic steady-state

$$V\frac{\partial w^n}{\partial t^*} + VD_t w^n + R(w^n) = 0.$$

D. Stabilty

In this section, the stability of the time spectral method will be examined. For simplicity, consider a one-dimensional space.

$$V\frac{\partial w^n}{\partial t^*} + V\sum_{m=-\frac{N}{2}+1}^{\frac{N}{2}-1} d_m w^{n+m} + A\frac{\partial w^n}{\partial x} = 0,$$

where A is the Jacobian of the spatial flux operator.
A Von-Neuman analysis of these equations using a single spatial fourier mode and a single time fourier mode gives

$$V\frac{\partial \hat{w}}{\partial t^*} + V\sum_{m=1}^{\frac{N}{2}-1} P_m \hat{w} + \frac{Q}{\Delta x}\hat{w} = 0$$

where $P_m = i\frac{2\pi}{T}2d_m sin(km\Delta t)$ is the spectral matrix corresponding to the physical time discretization, and with central differences for the spatial discretization, $Q = iAsin(w\Delta x)$.
Let $\bar{\lambda}$ denote the maximum eigenvalue of Q, and $\bar{\lambda}_r$, $\bar{\lambda}_i$ its real and imaginary parts. Then,

$$V\frac{\partial \check{w}}{\partial t^*} \leq -[\frac{\bar{\lambda}_r}{\Delta x} + (\frac{\bar{\lambda}_i}{\Delta x} + V\frac{2\pi}{T}\sum_{m=1}^{\frac{N}{2}-1} 2|d_m|)i]\check{w}$$

Note that the source term due to the time-spectral term affects only the imaginary part of the eigenvalue associated with the time averaged solution.

III. Results

This section provides an examination of the accuracy and efficiency of the proposed Time Spectral algorithm. Validation of the algorithm is provided by a comparison with experimental data and other numerical results.

A. Implementation

The method is implemented using a conservative cell-centered semi-discrete finite volume scheme. A full W-cycle multigrid algorithm is used for accelerating convergence, in which a pseudo time step with a five-stage Runge-Kutta scheme is performed at each level. Blended first and third order numerical fluxes are introduced to suppress spurious modes and ensure stability. Eddy viscosity for the RANS equations is modeled using an algebraic Baldwin-Lomax turbulence model, i.e. the turbulence is assumed to be steady.

The explicit nature of the time advancement scheme facilitates parallelization in space. Multiple blocks are distributed on different processors and the parallel implementation on the three-dimensional unsteady viscous code(FLO107) is done using the Message Passing Interface(MPI).[8]

Test Case	M_∞	α_m, $deg.$	Re_c, $(million)$	α_0, $deg.$	k_c	$pitching-axis$ $(\%chord_{root})$
AGARD CT6	0.796	0	12.56	1.01	.202	25
NLR LANN CT5	0.82	0.59	7.3	0.25	.102	62.1

Table 1. Characteristics of the test cases

B. Test Cases

Oscillatory pitching motion has been simulated for both two- and three-dimensional test cases. These computational results are compared with experimental data whose characteristics are specified in Table 1. The pitching motion of the airfoil/wing, a function of time, is of the form,

$$\alpha(t) = \alpha_m + \alpha_0 sin(\omega t),$$

where, α_m is the mean angle of attack, α_0 is the maximum amplitude of pitching, and ω, the angular velocity is given in terms of a non-dimensional parameter, the reduced frequency, k_c. Reduced frequency is defined as

$$k_c = (\omega l_c)/(2V_\infty).$$

Here l_c, the characteristic length is the root chord length. Reynolds number Re_c is based on the root chord and V_∞ is the free-stream velocity.

1. *Two-dimensional case*

In this section we present simulations of the oscillatory pitching airfoil AGARD CT6 (NACA 64A010) case, which has been widely studied.[6,9,4] This experimental test was conducted by Davis.[10]

In order to validate the time spectral method, the Euler equations are solved on a 160x32 O-mesh, automatically generated using a conformal mapping procedure. In addition, the RANS equations are solved on a 256x64 externally generated C-mesh. The near-field mesh resolution of both these meshes are shown in Fig.1. A grid convergence study has been done on this test case for both Euler and RANS calculations with similar spatial discretization by McMullen et.al.[6]

Time accurate solutions are obtained with N=4,8,12... time intervals, i.e. the time period of oscillation of the pitching airfoil is divided into N equal time intervals. This corresponds to representing (N/2) modes, the steady state and (N/2)-1 harmonics. Coefficient of lift(C_l) as a function of angle of attack based on Euler calculations is provided in Fig. 2(a). (The curve is generated using trigonometric interpolation.) A Navier-Stokes calculation on the same test case with similar temporal resolution shows a much better approximation to the experimental data as shown in Fig. 2(b). Furthermore, a temporal mode convergence is achieved as is evidenced by the minor deviation of the lift-alpha loop with variation in temporal resolution. Hence we have

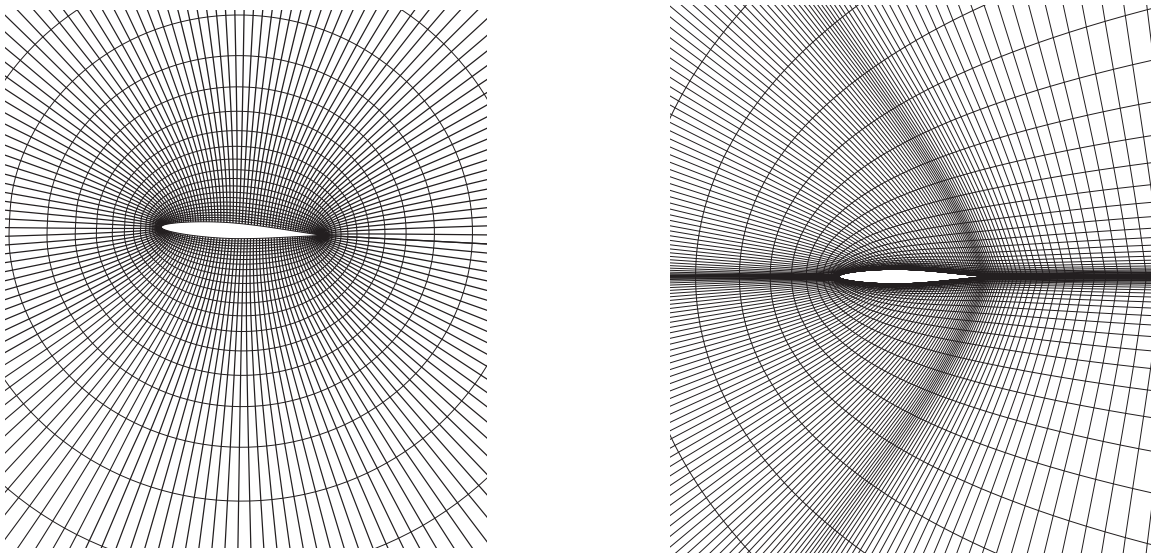

Figure 1. Near-field O- and C-mesh resolution

shown that 4 time intervals, or 1 harmonic is sufficient to obtain engineering accuracy for this oscillatory pitching airfoil.

Fig. 3(a) and 3(b) display the coefficient of moment (C_m) data as a function of angle of attack obtained from Euler and RANS calculations. The C_m data differs significantly from the experimental results. This is not surprising considering that previous investigators[9] using similar spatial discretizations have shown similar discrepancies between the experimental data and their time accurate computations.

Fig. 4 and Fig. 5 show the convergence histories of the Euler and RANS calculations for one of the time instances. With a 5-level W-cycle multigrid, the Euler calculation converges six orders of magnitude(RMS density residual) in 100 multigrid cycles and the RANS calculation converges five orders of magnitude in about 700 multigrid cycles.

2. Three-Dimensional Case

In this section, we present three-dimensional unsteady results. This test case relates to a semi-span model of a transport-type wing with a supercritical airfoil section, the LANN wing. Table (1) summarizes the characteristics of the central transonic test case CT5 of the experimental program conducted by R.J.Zwaan from NLR.[11]

Unsteady RANS calculations have been performed for flow over the oscillatory pitching LANN wing with a 256x64x48 internally generated C-H viscous mesh, based on a conformal mapping procedure. It should be noted that all computations have been carried out on the theoretical coordinates of the LANN wing, which

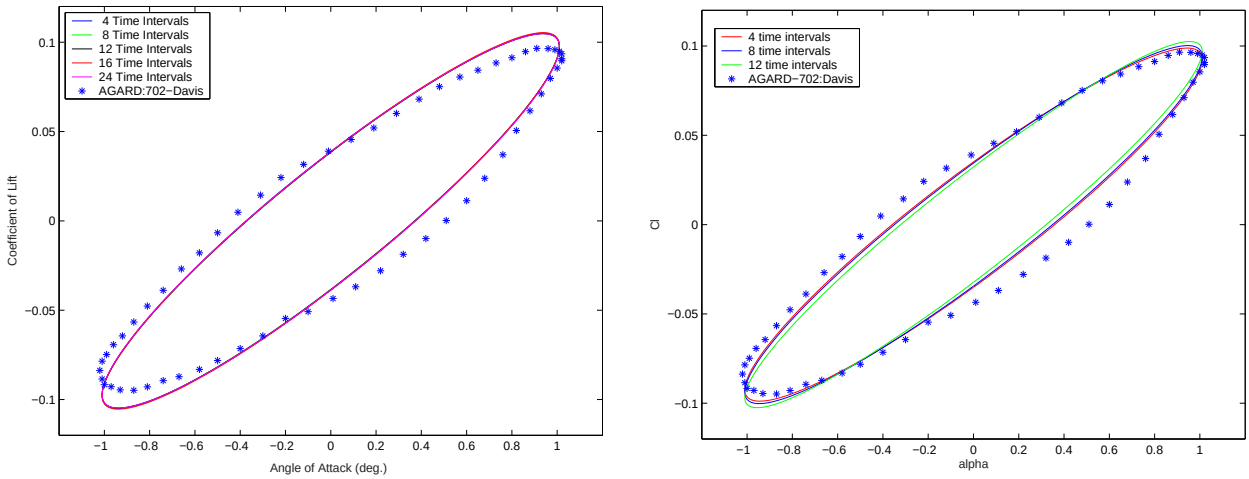

(a) Euler Calculations

(b) Navier-Stokes calculations

Figure 2. Comparison of C_l data with experimental results for the AGARD CT6 test case.

deviate from the measured coordinates. Fig. 6(a) and (b) display the pressure distribution at a 20% span section at $\alpha = \alpha_{mean}$ and $\alpha = \alpha_{max}$ respectively. Time spectral solutions with N=4,8 and 12 time intervals are displayed. Also displayed are the results from another numerical test conducted by DLR WB-AE.[12] They use a viscous-inviscid interaction(VII) method, which combines an inviscid(full potential method) and a boundary-layer method by an appropriate coupling approach.

The experiment shows a strong λ-type shock system which has been captured by the numerical results. The pressure peaks have been predicted well, but the location of the shock is not accurate. This could be attributed to the algebraic Baldwin-Lomax turbulence model. Note that the time spectral solution has converged in temporal resolution. Using 4 time intervals the flow physics has been captured to engineering accuracy. Fig. 7 (a) and (b) display a similar pressure distribution at 65% span location.

Fig. 8 shows the convergence history of the RANS calculation on the LANN pitching wing. With a 4-level W-cycle multigrid, the parallel code converges 5 orders of magnitude in 800 multigrid cycles.

C. Spectral Accuracy

In the previous sections, the time spectral method has been tested and verified with experimental and numerical results for simple pitching cases which are characterised by an amplitude and a phase. In these cases it has been shown that 4 time intervals are sufficient to successfully capture the unsteady phenomena. In this section, we will explore a case with a more complicated pitching history, one characterised by many frequencies.

We haven chosen a pitching cycle of the form

$$\alpha(t) = \frac{3}{5 - 4cos(t)},$$

Fig. 9 shows the variation of angle of attack, α, as a function of time for one full period. The time period is 2π. Euler calculations have been performed on the NACA64A010 160x32 O-mesh at free-stream $M_\infty = 0.796$ and pitched about 25% chord.

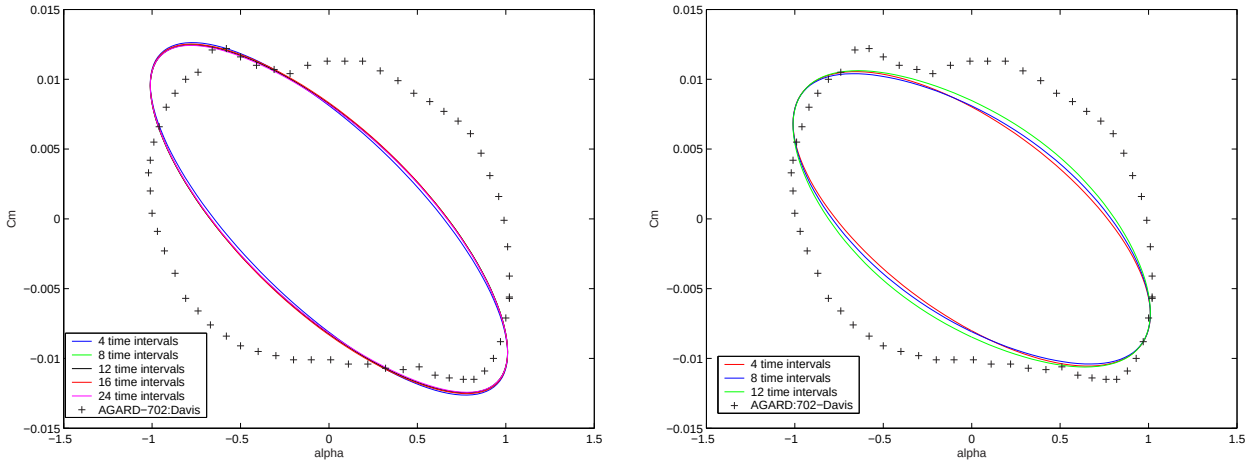

(a) Euler Calculations (b) Navier-Stokes calculations

Figure 3. Comparison of C_m data with experimental results for the AGARD CT6 test case.

Fig. 10(a) shows the variation of Coefficient of Lift(C_l) as a function of α computed with N=4,8,12,16,20 and 24 time intervals per pitching cycle. Note that at least 16 time intervals are required to obtain engineering accuracy. 4 time intervals are not sufficient, but increasing N shows an improvement in the solution and a convergence in the right direction. A similar trend is portrayed in Fig. 10(b) which displays the variation of coefficient of moment about the quarter chord, C_m, as a function of α. With higher-order spatial discretization, one may obtain spectral convergence in time.

IV. Conclusions and Future Work

The numerical results and their validation confirm the accuracy and computational efficiency of the Time Spectral Algorithm for unsteady periodic problems. The oscillatory pitching airfoil/wing case showed that engineering accuracy can be obtained with just four time intervals per period or one harmonic. A good prediction of the flow around a three-dimensional pitching wing has increased the range of problems that can be tackled with this method. Since periodicity is enforced, computational effort towards resolving the decay of initial transients in minimal. The need for only a small number time intervals to obtain sufficient accuracy for the globally integrated quantities together with the fact that spectral accuracy can be achieved with higher order spatial discretization, provides a promising route to more efficient computation of complex periodic unsteady problems.

The current implementation has an explicit treatment of the time derivative term. This works fine for small frequencies and small pitching amplitudes. An implicit treatment of the time derivative is under investigation for high frequency applications. A local time-stepping scheme based on the modified stability region, due to the time spectral source term, is also a topic of interest. The current unsteady implementation is very memory intensive, since all the time instances are solved for at the same time and need to be allocated simultaneously. Hence, an extension to a large number of time intervals for complex problems might be prohibitive. Nevertheless, this approach can be used with a small number of intervals to provide an initial guess for the standard BDF without having to evolve through transients, and hence provide a much faster periodic solution.

Such an efficient method could bring about significant benefits in a wide variety of applications. These include rotor-stator combinations in turbomachinery, helicopter rotors, aeroelastic problems, flapping wing

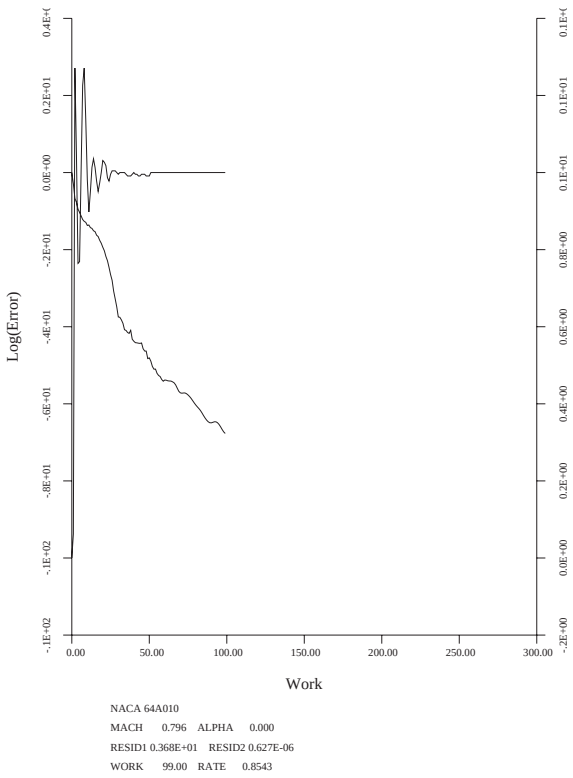

Figure 4. Convergence History - CT6 - Euler

flight, flow control by synthetic jets. The time spectral algorithm has already been implemented successfully for low RPM turbomachinery problems. This required a modification of the time spectral algorithm to conform to sector periodicity.[13] The algorithm has also been used for research in Vertical-Axis Wind-Turbines[14] to study the dynamic motion of a turbine blade spinning about an axis.

V. ACKNOWLEDGMENT

This work has benefited from the generous support of the Department of Energy under contract number LLNL B341491 as part of the Accelerated Strategic Computing Initiative(ASCI) program at Stanford University.

References

[1]A. Jameson and D.A. Caughey. How many steps are required to solve the euler equations of steady compressible flow: In search of a fast solution algorithm. *AIAA paper 01-2673*, 15th Computational Fluid Dynamics Conference, Anaheim, CA, June 2001.

[2]K.C. Hall, J.P. Thomas, and W.S. Clark. Computation of unsteady nonlinear flows in cascades using a harmonic balance technique. *AIAA Journal*, 40(5):879–886, May 2002.

[3]A. Jameson. Time dependent calculations using multigrid, with applications to unsteady flows past airfoils and wings. (*91-1596*), June 1998.

[4]J.M. Hsu and A. Jameson. An implicit-explicit hybrid scheme for calculating complex unsteady flows. *AIAA paper 02-0714*, AIAA 40th Aerospace Sciences Meeting and Exhibit, Reno, NV, January 2002.

[5]M. McMullen, A. Jameson, and J.J. Alonso. Acceleration of convergence to a periodic steady state in turbomachinery

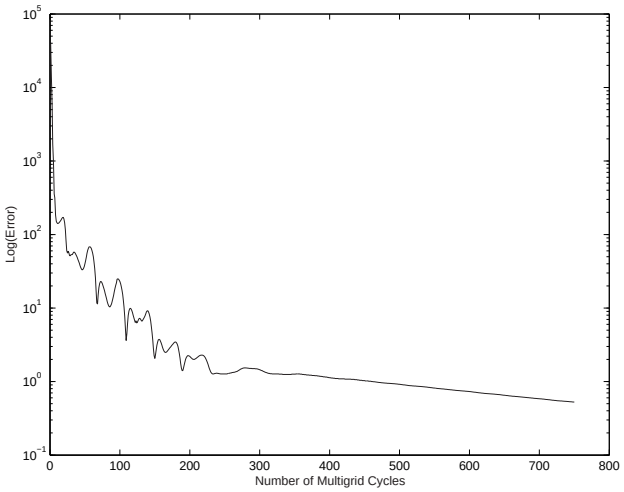

Figure 5. Convergence History - CT6 - RANS

flows. *AIAA paper 01-0152*, AIAA 39th Aerospace Sciences Meeting, Reno, NV, January 2001.

[6]M. McMullen, A. Jameson, and J.J. Alonso. Application of a non-linear frequency domain solver to the euler and navier-stokes equations. *AIAA paper 02-0120*, AIAA 40th Aerospace Sciences Meeting and Exhibit, Reno, NV, January 2002.

[7]A.Quarteroni C.Canuto, M.Y.Hussaini and T.A. Zang. *Spectral Methods in Fluid Dynamics; Springer Series in Computational Physics*. Springer Verlag, 1988.

[8]Message Passing Interface Forum. *MPI: A Message-Passing Interface Standard*, March 1994.

[9]N.A.Pierce and J.J. Alonso. Efficient computation of unsteady viscous flow by an implicit preconditioned multigrid method. *AIAA Journal*, 36:401–408, 1998.

[10]S.S. Davis. Naca 64a010 (nasa ames model) oscillatory pitching. *AGARD Report 702*, January 1982.

[11]R.J. Zwaan. Data set 9, LANN Wing. Pitching Oscillation. Technical report, AGARD, 1985. Agard-R-702 Addendum No.1.

[12]W.Haase, E.Chaput, E.Elsholz, M.A.Leschziner, and U.R.Muller. *ECARP: Validation of CFD Codes and Assessment of Turbulence Models; Notes on Numerical Fluid Mechanics, Vol. 58*. Vieweg, 1997.

[13]A. Gopinath, E. Van der Weide, and A. Jameson. Turbomachinery applications with the time spectral method. *AIAA (pending) paper*, 17th AIAA Computational Fluid Dynamics Conference, Toronto, Ontario, June 6-9 2005.

[14]J.C.Vassberg, A.Gopinath, and A.Jameson. Revisiting the vertical-axis wind-turbine design using advanced computational fluid dynamics. *AIAA paper 05-1220*, 43rd AIAA Aerospace Sciences Meeting and Exhibit, Reno, NV, January 10-13 2005.

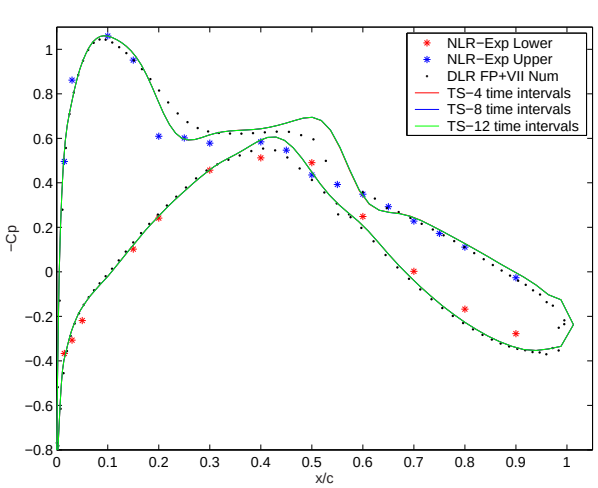

(a) $\eta = 20\%$, $\alpha = \alpha_{mean} = 0.59$ deg.

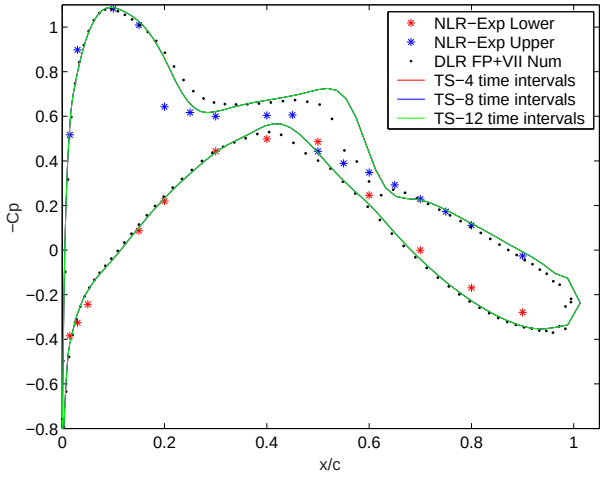

(b) $\eta = 20\%$, $\alpha = \alpha_{max} = 0.84$ deg.

Figure 6. Pressure Distribution At 20% Span : Verification with Experimental and a VII Numerical Method

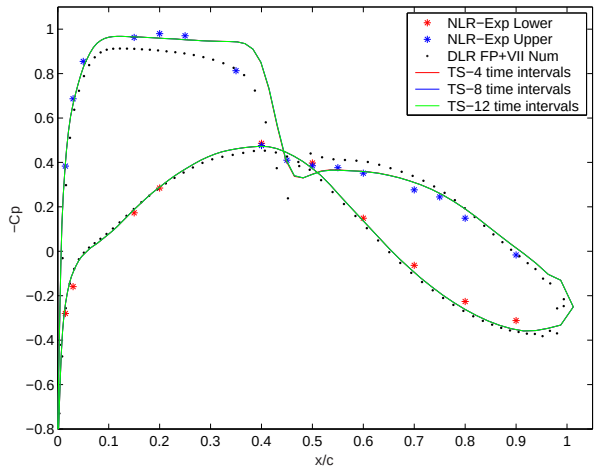

(a) $\eta = 65\%$, $\alpha = \alpha_{mean} = 0.59$ deg.

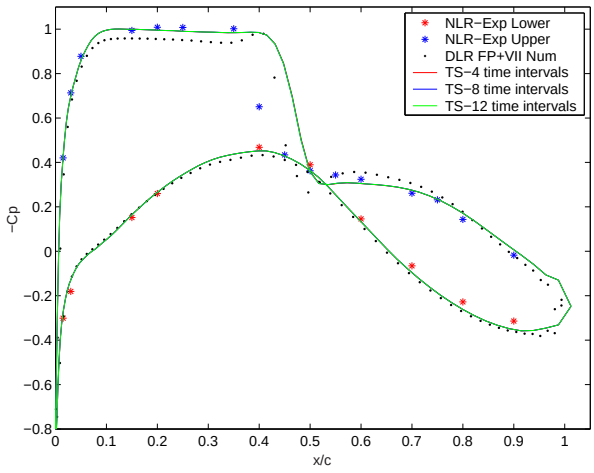

(b) $\eta = 65\%$, $\alpha = \alpha_{max} = 0.84$ deg.

Figure 7. Pressure Distribution At 65% Span : Verification with Experimental and a VII Numerical Method

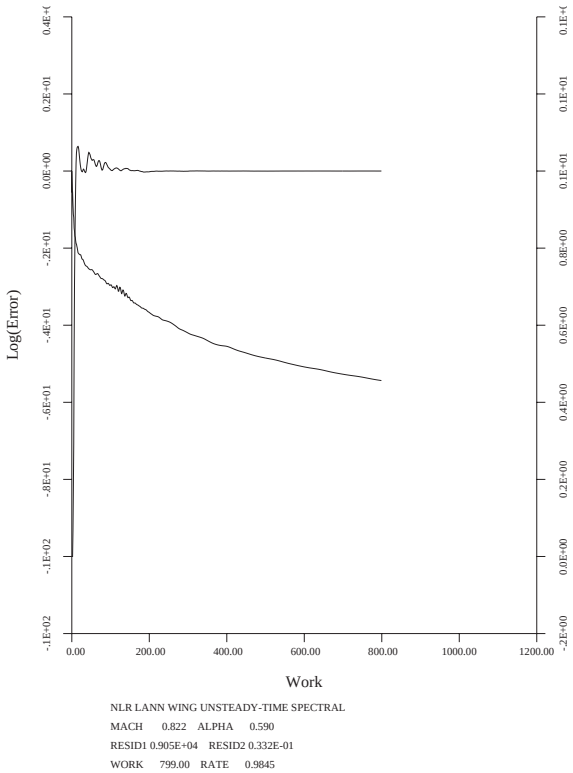

Figure 8. Convergence History - LANN - RANS

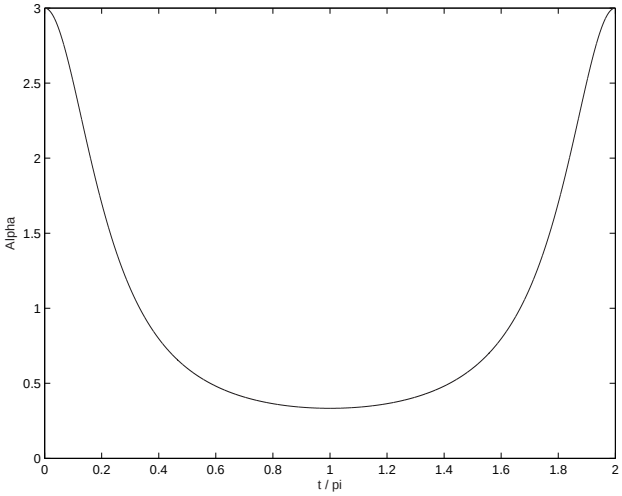

Figure 9. α as a function of time for one period. $\alpha = \frac{3}{5-4cos(t)}$

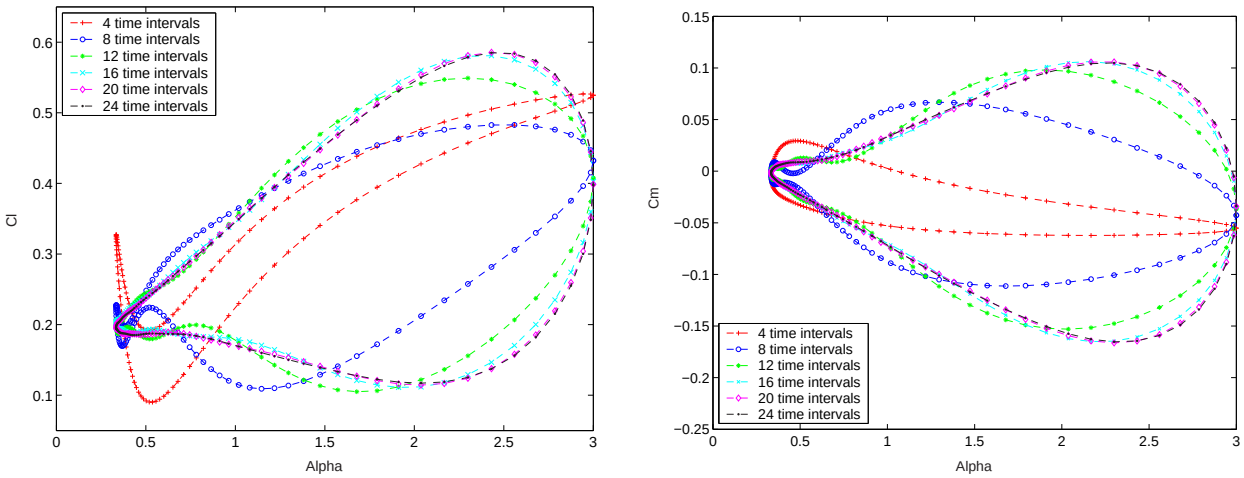

(a) C_l-α plot (b) C_m-α plot

Figure 10. Validation : C_l-α and C_m-α plots showing spectral convergence